Abundance Distributions Imply Elevated Complexity of Post-Paleozoic Marine Ecosystems

Peter J. Wagner, *et al.*

Science **314**, 1289 (2006);
DOI: 10.1126/science.1133795

Table 2. Comparison of mascon-derived trends with previous values determined from satellite and airborne altimetry (*3*). The mascon-derived trends were corrected for GIA and potential signal loss (~9%) as determined from simulation analysis (*14*). Errors computed as in (*14*) along with assuming 100% error in GIA.

Drainage system	2003–2005 mascon-derived ice mass trend (Gton/year)	1992–2002 altimeter-derived ice mass trend (*3*) (Gton/year)	Delta (2003–2005) – (1992–2002) (Gton/year)
1	8 ± 5	1.6 ± 0.3	6 ± 5
2	8 ± 4	8.8 ± 0.2	–1 ± 4
3	–25 ± 4	–4.9 ± 2.0	–20 ± 4
4	–77 ± 11	–15.7 ± 1.2	–61 ± 11
5	7 ± 13	11.4 ± 0.8	–5 ± 13
6	–22 ± 7	10.5 ± 0.5	–32 ± 7
Greenland	–101 ± 16	11.7 ± 2.5	–113 ± 17

al cycle for the low-elevation coastal regions and observing the summer melt and winter growth cycles. Our finding of an overall mass loss of 101 ± 16 Gton/year for 2003 to 2005 is consistent with the finding of near balance during the 1990s (*3*) and with the recent results on increased melt rates (*1*), acceleration of outlet glaciers (*5*, *20*), and the increasingly negative surface balance in recent years (*22*). The Greenland mass loss contributes 0.28 ± 0.04 mm/year to global sea level rise, which is nearly 10% of the 3 mm/year rate recently observed by satellite altimeters (*23*). The observed change from the 1990s of –113 ± 17 Gton/year represents a change from a small growth of about 2% of the annual mass input to a loss of about 20%, which is a significant change over a period of less than 10 years (*24*). This result is in very good agreement with the change in trend of –117 Gton/year from 1996 to 2005 determined from radar interferometry (*5*). During the 1990s, the observed thinning at the margins and the growth inland were both expected responses to climate warming. Our new results suggest that the processes of significant ice depletion at the margins, through melting and glacier acceleration, are beginning to dominate the interior growth as climate warming has continued.

References and Notes

1. An update of (*18*) posted at http://cires.colorado.edu/science/groups/steffen/greenland/melt2005 shows a 31% increase in mean melt area between 1979 and 2005.
2. W. Krabill *et al.*, *Geophys. Res. Lett.* **31**, L24402 (2004).
3. H. J. Zwally *et al.*, *J. Glaciol.* **51**, 509 (2005).
4. R. Thomas *et al.*, *Geophys. Res. Lett.* **33**, L10503 (2006).
5. E. Rignot, P. Kanagaratnam, *Science* **311**, 986 (2006).
6. O. M. Johannessen, K. Khvorostovsky, M. W. Miles, L. P. Bobylev, *Science* **310**, 1013 (2005); published online 20 October 2005 (10.1126/science.1115356).
7. For mass balance within the 1992–2002 time period, the following estimates have been published: +11 ± 3 Gton/year for 1992–2002 (*3*), –46 Gton/year for 1993/4 – 1998/9 (*21*), –72 ± 11 Gton/year for 1997–2003 (*2*), and –83 ± 29 and –127 ± 29 Gton/year for 1996 and 2000, respectively (*5*). If the correction for firn compaction used in the radar altimeter analysis (*3*) is applied to the airborne altimeter estimates (*2*, *4*, *21*), the difference between the two approaches is reduced by about 23 Gton/year, as reflected by revised airborne values of –4 to –50 Gton/year for 1993 to 1999 (*4*).
8. B. D. Tapley, S. Bettadpur, J. C. Ries, P. F. Thompson, M. M. Watkins, *Science* **305**, 503 (2004).
9. I. Velicogna, J. Wahr, *Science* **311**, 1754 (2006); published online 1 March 2006 (10.1126/science.1123785).
10. I. Velicogna, J. Wahr, *Geophys. Res. Lett.* **32**, L18505 (2005).
11. J. L. Chen, C. R. Wilson, B. D. Tapley, *Science* **313**, 1958 (2006); published online 10 August 2006 (10.1126/science.1129007).
12. D. Rowlands *et al.*, *Geophys. Res. Lett.* **32**, L04310 (2005).
13. S. B. Luthcke *et al.*, *Geophys. Res. Lett.* **33**, L02402 (2006).
14. Materials and methods are available as supporting material on *Science* Online.
15. H. J. Zwally, M. B. Giovinetto, *Ann. Glaciol.* **31**, 126 (2000).
16. W. R. Peltier, *Annu. Rev. Earth Planet. Sci.* **32**, 111 (2004).
17. G. Ramillien *et al.*, *J. Global Planet. Change* **53**, 10.1016/j.gloplacha.2006.06.003 (2006).
18. W. Abdalati, K. Steffen, *J. Geophys. Res.* **106**, 33983 (2001).
19. J. E. Box *et al.*, *J. Clim.* **19**, 2783 (2006).
20. G. Ekstrom, M. Nettles, V. C. Tsai, *Science* **311**, 1756 (2006).
21. W. Krabill *et al.*, *Science* **289**, 428 (2000).
22. E. Hanna *et al.*, *J. Geophys. Res.* **110**, D13108 (2005).
23. A. Cazenave, R. S. Nerem, *Rev. Geophys.* **42**, 10.1029/2003RG000139 (2004). An update is posted at http://sealevel.colorado.edu.
24. For the 1990s, we used the small 11 Gton/year mass gain from (*3*) and noted that the negative balances discussed in (*7*) either would give significantly less negative changes than 113 Gton/year or would give positive changes, in contradiction to the evidence for increases in melt and glacier accelerations. Also, our 113 ± 17 Gton/year is in good agreement with the change in mass flux of 117 Gton/year from 1996 to 2005 from radar interferometry (*5*).

25. We acknowledge NASA's Solid Earth and Natural Hazards Program, NASA's Cryospheric Sciences Program, and NASA's Ice, Cloud, and Land Elevation Satellite and GRACE missions for their support of this research and the quality of the GRACE Level 1B products produced by our colleagues at the Jet Propulsion Laboratory. We thank S. Klosko, T. Williams, and D. Pavlis for their many contributions and the reviewers for their astute commentary.

Supporting Online Material

www.sciencemag.org/cgi/content/full/1130776/DC1
Materials and Methods
Fig. S1

2 June 2006; accepted 10 October 2006
Published online 19 October 2006;
10.1126/science.1130776
Include this information when citing this paper.

Abundance Distributions Imply Elevated Complexity of Post-Paleozoic Marine Ecosystems

Peter J. Wagner,[1]* Matthew A. Kosnik,[2] Scott Lidgard[1]

Likelihood analyses of 1176 fossil assemblages of marine organisms from Phanerozoic (i.e., Cambrian to Recent) assemblages indicate a shift in typical relative-abundance distributions after the Paleozoic. Ecological theory associated with these abundance distributions implies that complex ecosystems are far more common among Meso-Cenozoic assemblages than among the Paleozoic assemblages that preceded them. This transition coincides not with any major change in the way fossils are preserved or collected but with a shift from communities dominated by sessile epifaunal suspension feeders to communities with elevated diversities of mobile and infaunal taxa. This suggests that the end-Permian extinction permanently altered prevailing marine ecosystem structure and precipitated high levels of ecological complexity and alpha diversity in the Meso-Cenozoic.

Marine ecosystem complexity is thought to have increased over the past 540 million years, in terms both of the alpha [i.e., local (*1*)] diversity of fossilized assemblages and of the numbers of basic ecological types (i.e., "guilds") (*2*–*5*). Ecological theory predicts that ecosystem complexity affects relative-abundance distributions (RADs) (*6*). Therefore, if fossiliferous assemblages adequately reflect original communities, then RADs implying interactions and/or a multiplicity of basic ecologies should become more common over time, and RADs implying simple partitioning and/or limited interaction should become less common. Taphonomic studies show that death assemblages can accurately reflect one aspect of RADs of skeletonized taxa within living communities, namely, rank-order abundance (*7*). Moreover, paleoecological

[1]Department of Geology, Field Museum of Natural History, 1400 South Lake Shore Drive, Chicago, IL 60605, USA. [2]School of Marine and Tropical Biology, James Cook University, Townsville, QLD 4811, Australia.

*To whom correspondence should be addressed. E-mail: pwagner@fmnh.org

studies can detect different model RADs (*8*, *9*). Both findings suggest that the fossil record can test the proposition that marine community structure changed over the Phanerozoic.

RAD evenness (i.e., uniformity of abundances in an assemblage) is greater in the Meso-Cenozoic than in the Paleozoic, which is expected if alpha diversity of Meso-Cenozoic communities is generally greater than that of Paleozoic communities (*4*). However, evenness is only one aspect of a RAD. Different ecological models for community assembly make more explicit predictions about specific RAD types found in natural communities: (i) geometric or log-series: species entering a community preempt a remaining portion of the available resources without increasing the total resources in the ecosystem (*10*); (ii) zero-sum multinomial: intrinsic properties affecting migration, origination, and extinction rates affect RADs rather than do ecological interactions among species (*11*); (iii) Zipf or lognormal: new species increase ecospace, either by facilitating opportunities for additional species (*12*) or by niche construction (*13*); and (iv) lognormal: multiple diverse guilds (i.e., groups playing similar general ecological roles) each have their own distributions, but the pool of these distributions is lognormal (*6*).

Scenarios (iii) and (iv) both require more numerous ecological processes and allow for greater varieties of taxa than do scenarios (i) and (ii). Thus, a shift from ecologically "simple" RADs (i.e., geometric or zero-sum) to ecologically "complex" RADs (i.e., Zipf or lognormal) should accompany an increase in ecological and alpha diversity.

We examined 1176 fossiliferous assemblages of macroinvertebrate marine species with abundance data from the Paleobiology Database (*14*) to determine whether the frequency of model RADs among Meso-Cenozoic assemblages differs from those of Paleozoic assemblages in a manner consistent with either increased interactions among species shaping community structure and/or elevated diversity of ecological guilds. For each assemblage, we determined the most likely representatives among the four general RAD models [fig. S3 (*15*)] based on the probability of observing X species with 1… *n* specimens given a sample size of *n* [fig. S4]. We then assessed the models using Akaike's weights based on Akaike's modified information criterion [AICc (*16*)]. We rejected alternative hypotheses if the weight of one hypothesis was 0.89 or greater (*17*).

Geometric and lognormal are the most common RADs. Considering just these two RADs, geometrics best fit Paleozoic assemblages about as frequently as lognormals do. However, geometrics best fit Meso-Cenozoic assemblages about one-quarter as frequently as lognormals do (Fig. 1A). Limiting the analyses to the 681 significant assemblages given Akaike weights and comparing just simple versus complex RADs shows that, whereas simple and complex assemblages are equally common in the Paleozoic, complex RADs typically are three to four times as common as are simple RADs in the Meso-Cenozoic (Fig. 1B) (*18*). The Cambrian might represent a third ratio of simple:complex assemblages. However, few Cambrian assemblages include 10+ taxa, which results in a small number of analyzed assemblages and thus large support bars that overlap those of other Paleozoic periods. Thus, we cannot currently reject the null hypothesis of a consistent Paleozoic ratio.

Because we are examining preserved assemblages rather than original communities, we must consider factors other than original community structure that might account for these results. Numbers of specimens per collection do not differ markedly between analyzed Paleozoic and Meso-Cenozoic collections, which precludes some methodological artifact based on sample size (Fig. 2A) (*19*). The numbers of classes per analyzed collection typically are higher for Paleozoic collections than for Meso-Cenozoic ones, which contradicts the idea of single-taxon Paleozoic lists implying overly simple RADs (Fig. 2B). Lithified rocks discourage the sampling of small and aragonitic specimens. Similarly, siliciclastic and carbonate sediments represent both different preservation and general ecological regimes, and siliciclastic sediments become decreasingly common over the Phanerozoic (*20*).

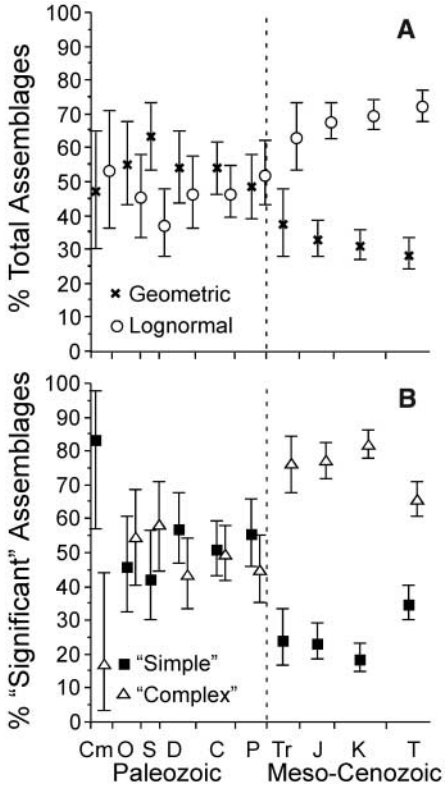

Fig. 1. Proportions of assemblages that best fit different RAD models. Error bars give one unit of support (*18*); if support bars do not overlap for the same model(s), then we reject the idea of the same proportions in those intervals. Dashed line separates Paleozoic from Meso-Cenozoic. (**A**) Results for all assemblages showing percentages that fit geometric better than lognormal and vice-versa. (**B**) Results from the 681 significant assemblages where the combined Akaike weights of the two simple (geometric or zero-sum multinomial) or two complex (Zipf or lognormal) models exceed 0.89.

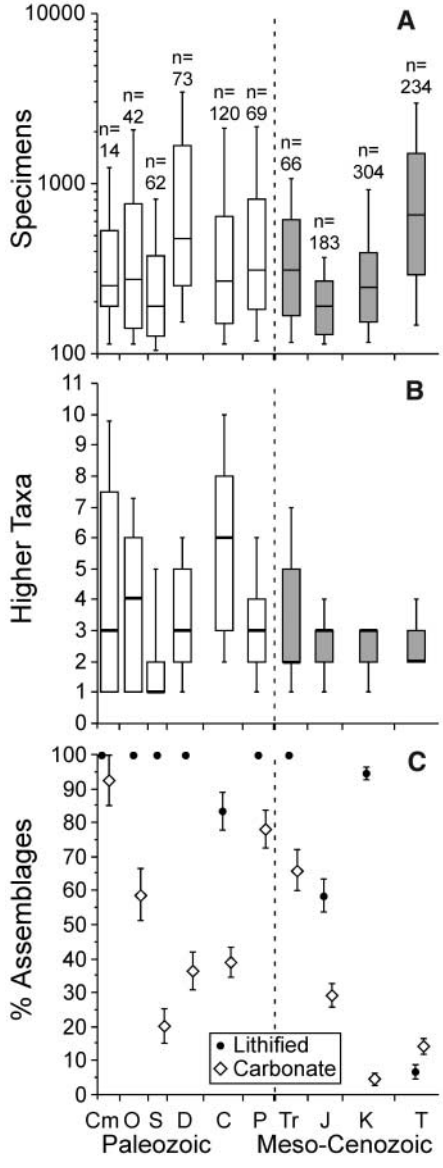

Fig. 2. Distributions of potential biasing factors over time. Box plots in (A) and (B) encompass 50% and error bars encompass 90% of the data. (**A**) Average numbers of specimens per analyzed assemblage. n, number of assemblages in each geologic period. (**B**) Number of classes present in assemblages. (**C**) Proportions of general preservational and environmental types with binomial error bars (*19*). "Lithified" gives proportions of analyzed assemblages identified as "lithified" rather than "poorly lithified" or "unlithified." "Carbonate" gives the proportions of analyzed assemblages with carbonate rather than siliciclastic or mixed siliciclastic/carbonate sediments. Lithification and basic sediment type can vary independently.

However, the shifts in lithified collections and siliciclastic/carbonate collections do not coincide with the RAD transition (Fig. 2C). Finally, analyses restricted to any one of these partitions replicate the overall pattern (tables S1 to S3 and figs. S5 to S8).

Worker bias also is unlikely given that the assemblages reflect 190 different studies and no single worker or study dominates the whole of either the Paleozoic or Meso-Cenozoic. Shifts in other taphonomic patterns, such as elevated preservation potential of aragonitic skeletons, happen after the Jurassic (*21*). Our study necessarily omits nonskeletonized organisms that contributed to the original RADs. However, the random removal of taxa from particular RADs tends to encourage a lognormal distribution as well as reduce test power, and thus biases the results against our findings. Moreover, there is no a priori reason to assume that frequencies of soft-bodied organisms occupying the same general habits as skeletonized organisms differed markedly between the Paleozoic and Meso-Cenozoic.

With little support for nonbiological explanations for differences between Paleozoic and post-Paleozoic RAD, our results imply a change in general structure. Ecological theory provides at least two nonexclusive explanations for the shift in RADs, both of which imply elevated ecological complexity in the Meso-Cenozoic. One is a higher diversity of basic ecological guilds in the Meso-Cenozoic (*2*, *3*). Even if taxa within different ecological guilds partition ecospace simply, then averaging across different distributions typically yields a lognormal distribution. Log-series, which are nearly identical to geometrics, better fit RADs for Cenozoic foraminifera in most cases than do lognormals (*9*), which corroborates this idea.

A second explanation is that guilds and/or taxa that become diverse in the Meso-Cenozoic are more prone to complex RADs. Mobile epifaunal and infaunal macroinvertebrates (especially bivalves and gastropods) that actively seek out nutrients typify major Meso-Cenozoic guilds, whereas sessile organisms (especially brachiopods) that filter nutrients suspended above the sediment-water interface typify major Paleozoic guilds (*2*, *5*). The former taxa also tend to be metabolically buffered from the physical environment to a much greater extent than do the latter taxa (*5*). Notably, this transition marks a change in dominance as well as in richness (*22*). For example, "modern" infaunal bivalves and carnivorous gastropods that so pervade later benthic assemblages also occur in the Paleozoic, where they are seldom diverse or common even in collections preserving aragonitic shells. Actively mobile taxa might be more apt to increase ecospace usage either by creating additional ecological opportunities for other taxa or through niche construction and more complex interaction webs than are sessile suspension feeders such as brachiopods or crinoids (*13*, *23*). Indeed, common Meso-Cenozoic sessile suspension feeders such as reef-building corals engineer their environments extensively, whereas living brachiopods and crinoids do not. Similarly, high-metabolism, environmentally buffered organisms might be more capable of inserting themselves into more varied ecosystems. A weak positive correlation does exist between the proportion of specimens that are mollusks and the Akaike weight of the complex RADs among the 43 Paleozoic assemblages with 10+ mollusk species and 100+ mollusk specimens. This is consistent with the idea that molluscan ecology helps drive the pattern. However, sessile brachiopods often dominated Triassic and even Jurassic ecosystems, which is inconsistent with this idea (*24*).

Increasing frequencies of "complex" RADs have implications for why sampled and inferred alpha diversity apparently increase over the Phanerozoic (*4*, *25*). We typically expect to sample fewer taxa from geometric RADs than from lognormal or Zipf RADs, even when all other parameters (true richness, sample size, and evenness) are the same (*26*). This might imply that Paleozoic faunas have a greater potential for hiding species than do Meso-Cenozoic ones. However, this mathematical possibility is biologically implausible. Among the 143 Paleozoic assemblages that best fit a geometric RAD, the median model posits 22 taxa with abundance frequencies (f) $\geq 10^{-4}$. This requires thousands of individuals to have even a small population of a 22nd taxon. Among the 376 Meso-Cenozoic assemblages that best match a lognormal RAD, the median model posits 84 taxa with $f \geq 10^{-4}$. Even if one limits comparisons to lognormal assemblages, then one finds that the median parameters posit only 35 taxa with $f \geq 10^{-4}$ for the 122 Paleozoic assemblages that best match the lognormal RAD. Thus, the shift from the Paleozoic to the post-Paleozoic world involves an increase in basic alpha diversity as well as in the frequency of RADs implying complex ecosystems.

Finally, the change in typical RADs coincides with the end-Permian extinction. Our results are consistent with evidence that this mass extinction drastically reorganized the marine ecosystem (*27*). In particular, the results are consistent with proposals for especially catastrophic causal mechanisms (*28*) and drastic reorganizations of marine ecosystem structure after the extinction (*2*, *29*). The shift to common "complex" RADs also offers an explanation for the change from extinction-driven to origination-driven diversity dynamics (*30*). If taxa that require "openings" in ecospace predominate, then diversification should be tied to extinction enabling incipient species to become established. Conversely, if predominant taxa tend to increase interactions and create ecological opportunities for (or facilitate the ecological persistence of) other taxa, then diversification should be a product of the frequency at which incipient species appear and the probability of those species creating a new niche and/or fitting into a potentially open one. Because generic diversification should reflect underlying species diversification, the shift in dominant taxa would affect not just RADs but also macroevolutionary dynamics. Thus, the end-Permian seemingly altered not just taxonomic diversity (*27*) but also predominant evolutionary and ecological dynamics.

References and Notes

1. R. H. Whittaker, *Taxon* **21**, 213 (1972).
2. R. K. Bambach, in *Biotic Interactions in Recent and Fossil Benthic Communities,* M. Tevesz, P. L. McCall, Eds. (Plenum, New York, 1983), pp. 719–746.
3. W. I. Ausich, D. J. Bottjer, in *Phanerozoic Diversity Patterns-Profiles in Macroevolution,* J. W. Valentine, Ed. (Princeton University Press, Princeton, NJ, 1985), pp. 255–274.
4. M. G. Powell, M. Kowalewski, *Geology* **30**, 331 (2002).
5. R. K. Bambach, A. H. Knoll, J. J. Sepkoski Jr., *Proc. Natl. Acad. Sci. U.S.A.* **99**, 6854 (2002).
6. J. S. Gray, in *Organization of Communities Past and Present,* J. H. R. Gee, P. S. Gillier, Eds. (Blackwell, Oxford, 1987), pp. 53–67.
7. S. M. Kidwell, *Science* **294**, 1091 (2001).
8. T. D. Olszewski, D. H. Erwin, *Nature* **428**, 738 (2004).
9. M. A. Buzas, L.-A. C. Hayek, *Paleobiology* **31**, 199 (2005).
10. R. B. Root, *Ecol. Monogr.* **37**, 317 (1967).
11. S. P. Hubbell, *The Unified Neutral Theory of Biodiversity and Biogeography* (Princeton University Press, Princeton, NJ, 2001).
12. S. Frontier, in *Oceanography and Marine Biology: An Annual Review*, M. Barnes, Ed. (Aberdeen Univ. Press, Aberdeen, 1985), pp. 253–312.
13. K. N. Laland, F. J. Odling-Smee, M. W. Feldman, *Proc. Natl. Acad. Sci. U.S.A.* **96**, 10242 (1999).
14. Paleobiology Database, http://paleodb.org. See (*31*).
15. Materials and methods are available as supporting material on *Science* Online.
16. AICc = -2 lnL(Hypothesis) + $2K[n/(n - K - 1)]$, where K is the number of parameters and n is the number of data points (*32*). This is identical to AIC(Hypothesis) + $[2K(K + 1)]/(n - K - 1)$. Akaike's weight (w_i) for each hypothesis is, $w_i = (e^{-\Delta i/2})/\sum(e^{-\Delta j/2})$, where Δ is the difference between the AICc of the best hypothesis and the hypothesis i.
17. The individual "weight" of each hypothesis is proportional to the probability of the data given that hypothesis, slightly modified by the number of parameters and data points (*33*). The cutoff of 0.89 is akin to the likelihood testing criterion of rejecting hypotheses when an outcome is eight times (or more) less probable for one hypothesis than for another.
18. A. W. F. Edwards, *Likelihood, Expanded Edition* (Johns Hopkins Univ. Press, Baltimore, 1992).
19. D. M. Raup, in *Analytical Paleobiology*, N. L. Gilinsky, P. W. Signor, Eds. (Paleontological Society, Knoxville, TN, 1991), vol. 4, pp. 136–156.
20. L. J. Walker, B. H. Wilkinson, L. C. Ivany, *J. Geol.* **110**, 75 (2002).
21. M. Kowalewski *et al.*, *Paleobiology* **32**, 533 (2006).
22. M. E. Clapham *et al.*, *Palaios* **21**, 431 (2006).
23. P. D. Roopnarine, *Paleobiology* **32**, 1 (2006).
24. M. Aberhan, *Palaios* **9**, 516 (1994).
25. A. M. Bush, R. K. Bambach, *J. Geol.* **112**, 625 (2004).
26. M. A. Kosnik, P. J. Wagner, *Evol. Ecol. Res.* **8**, 197 (2006).
27. D. H. Erwin, *Extinction: How Life on Earth Nearly Ended 250 Million Years Ago* (Princeton Univ. Press, Princeton, NJ, 2006).
28. A. H. Knoll, R. K. Bambach, D. E. Canfield, J. P. Grotzinger, *Science* **273**, 452 (1996).
29. M. L. Fraiser, D. J. Bottjer, *Comptes Rendus Palevol* **4**, 583 (2005).
30. M. Foote, *Paleobiology* **32**, 345 (2006).
31. Species data were downloaded on 6 November 2005. We limited analyses to marine assemblages with at least 100 specimens and at least 10 invertebrate taxa. The collections reflect 190 publications.

32. K. P. Burnham, D. R. Anderson, *Model Selection and Inference: A Practical Information-Theoretic Approach* (Springer, New York, ed. 2, 2002).
33. R. Royall, *Statistical Evidence: A Likelihood Paradigm* (Chapman and Hall, London, 1997).
34. T. D. Olszewski provided computer code to calculate zero-sum multinomials. R. Bambach, M. Foote, D. Jablonski, S. K. Lyons, and J. McElwain provided critical comments. W. Kiessling and M. Kowalewski provided valuable reviews. P.J.W.'s contributions were funded in part by NSF grant EAR-0207874. This is PBDB publication #48.

Supporting Online Material
www.sciencemag.org/cgi/content/full/314/5803/1289/DC1

Materials and Methods
Figs. S1 to S8
Tables S1 to S3
References

14 August 2006; accepted 2 October 2006
10.1126/science.1133795

Two Dobzhansky-Muller Genes Interact to Cause Hybrid Lethality in *Drosophila*

Nicholas J. Brideau,* Heather A. Flores,* Jun Wang,* Shamoni Maheshwari, Xu Wang, Daniel A. Barbash†

The Dobzhansky-Muller model proposes that hybrid incompatibilities are caused by the interaction between genes that have functionally diverged in the respective hybridizing species. Here, we show that *Lethal hybrid rescue* (*Lhr*) has functionally diverged in *Drosophila simulans* and interacts with *Hybrid male rescue* (*Hmr*), which has functionally diverged in *D. melanogaster*, to cause lethality in F1 hybrid males. LHR localizes to heterochromatic regions of the genome and has diverged extensively in sequence between these species in a manner consistent with positive selection. Rapidly evolving heterochromatic DNA sequences may be driving the evolution of this incompatibility gene.

Plant and animal hybrids are often sterile or lethal as a result of interspecific genetic divergence. The Dobzhansky-Muller model proposes that hybrid incompatibilities (HIs), which contribute to speciation, evolve as a consequence of interactions between or among genes that have diverged in each of the hybridizing species (*1*). Dobzhansky-Muller incompatibility genes require three criteria: Each gene reduces hybrid fitness, has functionally diverged between the hybridizing species, and depends on the partner gene to cause HI (Fig. 1A). Major-effect HI genes have been discovered, and functional divergence of single genes has been demonstrated by genetic tests (*2*, *3*) or suggested by patterns of molecular evolution (*4*). Although HI systems composed of complementary factors have been described (*5*, *6*) and interacting genomic regions of hybridizing species identified (*7*–*9*), no pair of Dobzhansky-Muller genes has been reported. It remains unclear whether HI phenotypes can be explained even in part by two-locus interactions, or alternatively whether HIs require complex multilocus interactions (*10*–*12*).

Interspecific crosses of *D. melanogaster* females to *D. simulans* males produce no sons.

Department of Molecular Biology and Genetics, Cornell University, Ithaca, NY 14853, USA.

*These authors contributed equally to this work.
†To whom correspondence should be addressed. E-mail: dab87@cornell.edu

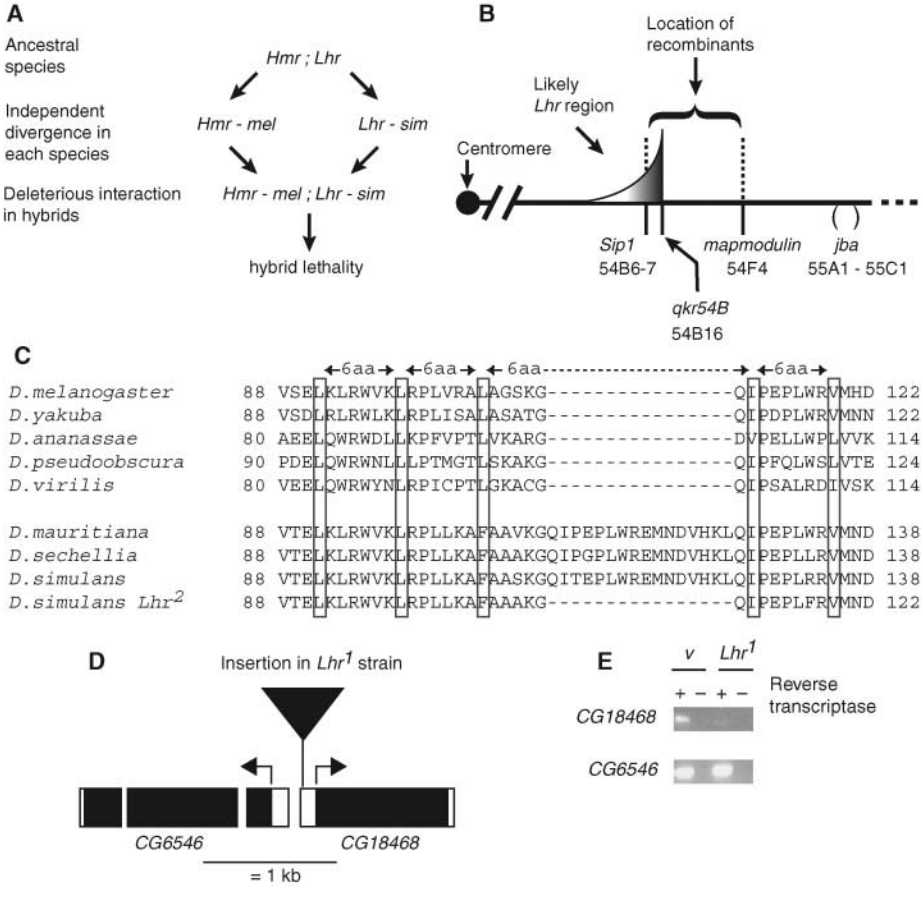

Fig. 1. *CG18468* encodes *Lhr*. (**A**) Model of *Hmr* and *Lhr* functional divergence and the interaction that causes hybrid lethality. Lethality results from the interaction between the *D. melanogaster Hmr* allele (*Hmr-mel*) and the *D. simulans Lhr* allele (*Lhr-sim*). (**B**) Map of *Lhr* region in *D. simulans*. Genetic markers and estimated cytological locations in *D. melanogaster* are shown below the line. Ten recombinants between *jba* and *Lhr* were selected and cross-overs mapped within a region of approximately 480 kb; the most proximal recombinant was between *Sip1* and *qkr54B* (diagram not to scale). (**C**) *CG18468* has a characteristic leucine zipper-like structure in all *Drosophila* species except *D. simulans*, *D. mauritiana*, and *D. sechellia*, which have a 16–amino acid insertion; this insertion is lacking in the *D. simulans* rescue strain Lhr^2. (**D**) Map of *CG18468* region at 54B7 and insertion in the Lhr^1 strain. Black boxes, coding regions; unfilled boxes, UTRs; arrows, predicted translation start sites. The large triangle represents an insertion of ~4 kb (triangle not to scale) located between nucleotides 11 and 13 of the predicted *CG18468* mRNA in Lhr^1. (**E**) The insertion in Lhr^1 reduces the level of mRNA of *CG18468* but not of *CG6546*. RT-PCR with larval RNA from a *vermillion* (*v*)–marked *D. simulans* strain and from the Lhr^1 strain.